Electronic Supplementary Material (ESI) for Nanoscale.

Supporting information

3D Superstructures with Orthorhombic Lattice Assembled by Colloidal PbS Quantum Dots

Elena V. Ushakova, Sergei A. Cherevkov, Aleksandr P. Litvin, Peter S. Parfenov, Igor A. Kasatkin, Anatoly V. Fedorov, Yurii K. Gun'ko, Alexander V. Baranov

S1. SAXS Experimental setup

The CuKα radiation at 1.54 Å wavelength and a Ni filter was used as an excitation. As a cuvette a thin layer of mica with Teflon ring on it was used. Due to the location of X-ray source and a detector on the vertical axis an investigation of QD colloidal solution in such a cuvette and process of solvent evaporation became possible. The advantage of this SAXS signals registration geometry is the possibility of recording the scattered radiation near the reference beam up to 0.1 deg. Using common "horizontal" geometry of the source and the detector arrangement the minimal angle that can be recorded is determined by the size, particularly the height difference of structure on the substrate. The cuvette compartment has a 2 mm gap allowing the solvent evaporate very slowly, thus allows us to achieve supercrystal growth by slow evaporation of saturated QD solution by open method. Evaporation time of the QD colloidal solution of 300-500 ul volume varies from 3 to 7 days.

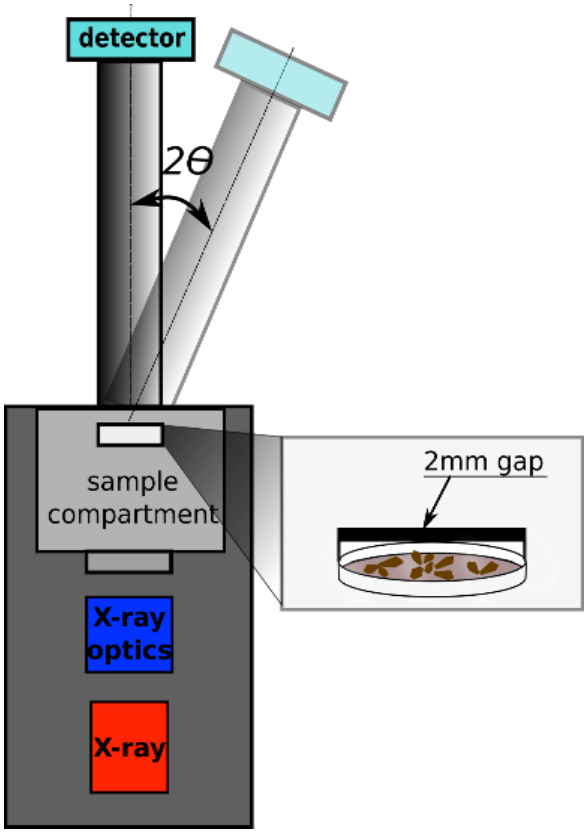

Figure S1 – Schematic image of SAXS measurement setup

S2. PbS CQD synthesis

Chemicals:

Lead oxide (PbO, >99.9%), bis(trimethylsilyl) sulfide (synthesis grade), oleic acid (OA, 90%), 1-octadecene (1-ODE, 90%), and tetrachloromethane (TCM, >99.5%, for IR spectroscopy) were used as purchased from Aldrich.

Synthesis:

Nanocrystals were prepared by the synthesis described in Ref. [Ushakova, E.V., et al. ACS Nano 6.10 (2012): 8913]. Briefly, 1 mmol of PbO, 4 mmol of OA, and 10 mL of 1-ODE were placed in the three-neck 25-ml flask, heated to 170°C and evacuated for 30 min to obtain a clear solution. Next, at 100°C 0.2 mmol of bis(trimethylsilyl) sulfide in 0.5 mL of 1-ODE was injected into the reaction vessel. The reaction mixture was additionally stirred for 1-15 min at 70°-100°C to grow nanocrystals of the range of sizes from 2.7 to 8.8 nm. The temperature of final solution was then lowered to 50° 60°C, and the QDs were precipitated by isopropanol. The obtained QDs were purified by dispersing in TCM with excess amount of isopropanol twice and redispersed in TCM for further experiments.

S3. ABS and PL spectra, PL decay of CQD in TCM solution

In Figure S3 ABS and PL spectra of CQD solutions in TCM are shown. In Table S3 the ABS and PL peak parameters are listed with calculated mean CQD size and its distribution.

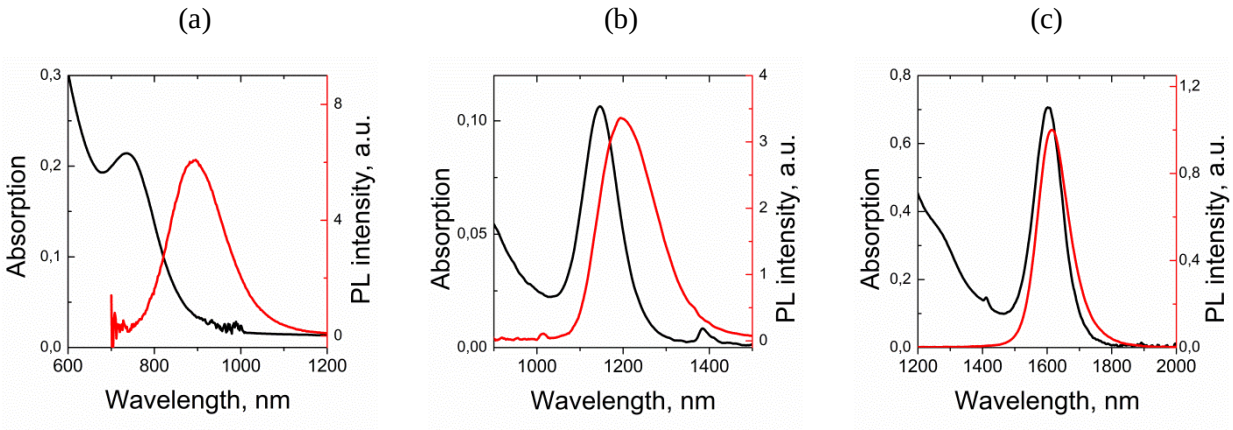

Figure S3 – ABS (black) and PL (red) spectra of QDs in TCM with size of: (a) 2.7 nm, (b) 4.6 nm, (c) 6.7 nm.

The mean CQD diameter was calculated by empirical formula according to Ref [Ushakova, E.V., et al. ACS Nano 6.10 (2012): 8913]:

$$D = 7.2 \cdot 10^{-10} \cdot \lambda^3 - 1.7 \cdot 10^{-6} \cdot \lambda^2 + 5.7 \cdot 10^{-3} \cdot \lambda - 0.9, \quad (1)$$

where D is mean CQD diameter in nm, λ is the ABS peak position in nm.

Table S3. Optical properties of CQDs of different sizes

Sample name	ABS peak position, nm	PL peak position, nm	PL lifetime, us	Calculated QD diameter, nm	QD size distribution from ABS spectra, %
$CQD_{2.7}$	740	895	1.6	2.7	11
$CQD_{4.6}$	1160	1270	1.62	4.6	4
$CQD_{6.7}$	1590	1620	0.67	6.7	4

S4. CQD monodispersity

In Figure S4 SAXS patterns from CQD solutions at first stage of the TCM evaporation are shown.

(a) (b)

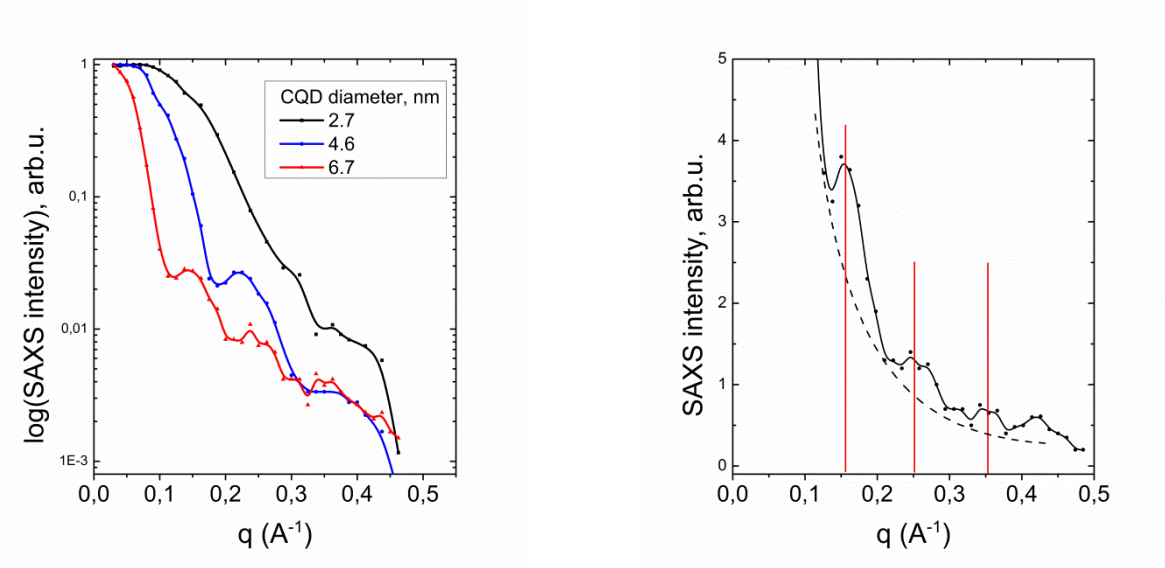

Figure S4 – (a) SAXS patterns from PbS CQDs in TCM. CQD diameters are shown in legend. (b) Zoomed part of SAXS pattern for $CQD_{6.7}$ with positions of side maxima

These signals can be fitted by Guinier approximation [Porod, G.; Glatter, O.; Kratky, O. Small Angle X-ray Scattering; Academic Press: London, 1982; 515 p.]:

$$I(q) = I_0 \exp\left(q^2 r_g^2/3\right), \quad (2)$$

where $q = (4\pi/\lambda)\sin(\theta/2)$ is a wave vector of scattering light with wavelength λ, θ – scattering angle, r_g – particle radius of gyration. From SAXS patterns the form, diameter and size distribution of CQDs and their mutual arrangement can be estimated. It is found that all PbS QDs have spherical form. CQD diameters are calculated by equation (2) and listed in Table S4. SAXS patterns contain side maxima, corresponding to the CQD size distribution. As one can see from SAXS patterns in Figure S4(a) with decreasing the CQD diameter side maxima become blurred. This fact indicates that the CQD monodispersity increases with the CQD diameter.

Table S4. Calculated CQD diameters

Sample name	Calculated from SAXS pattern QD diameter, nm	Calculated from ABS spectra PbS [S7], nm
$CQD_{2.7}$	2.4±0.3	2.7
$CQD_{4.6}$	4.4±0.2	4.6
$CQD_{6.7}$	6.6±0.1	6.7

S5. OA molecules amount in initial and treated $CQD_{6.7}$

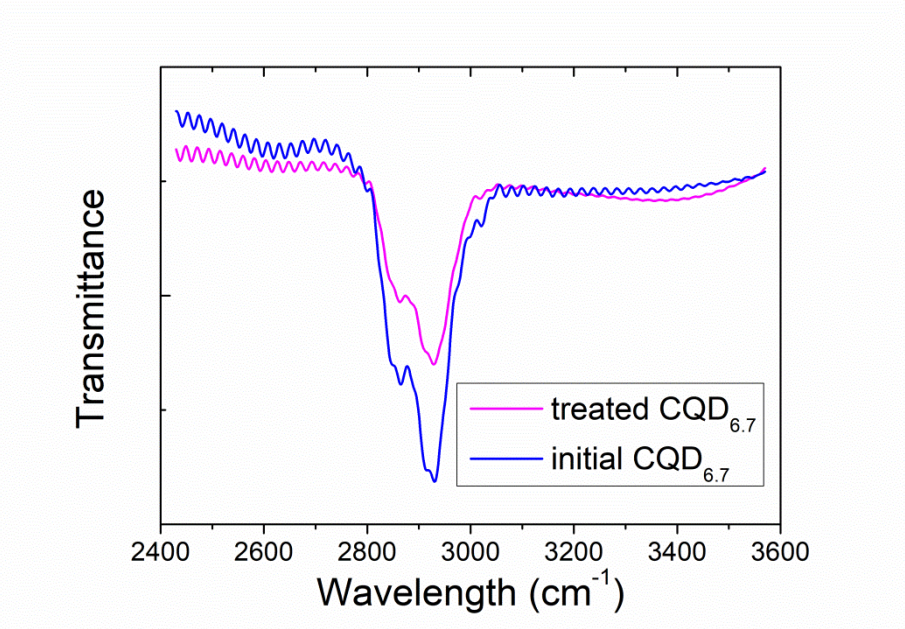

Figure S5 – FTIR spectra of $CQD_{6.7}$: initial QD solution (blue), treated with acetone (magenta)

S6. SAXS patterns from sample $SS_{2.7}$

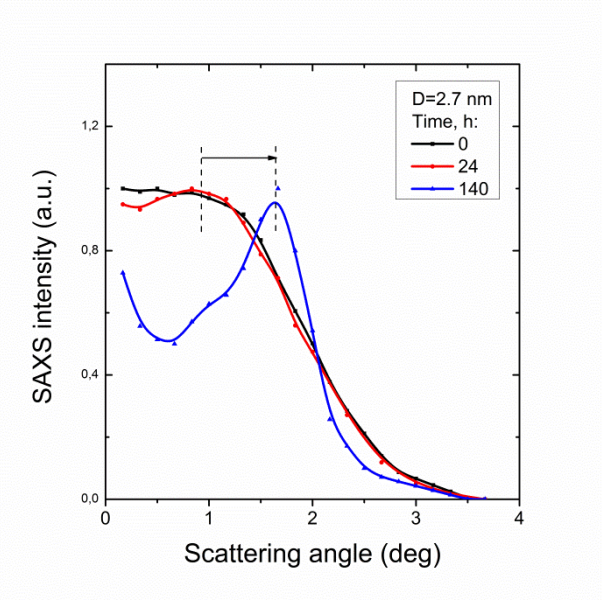

Figure S6 – SAXS patterns from sample $SS_{2.7}$: at first stage of the solvent evaporation (black line), after 24 h (red line) and 140 h (blue line) of the evaporation

S7. Indexing of SAXS patterns for $SS_{4.6}$ and $SS_{6.7}$.

For the indexing procedure in the software obtained spectra were scaled to the wide-angle region. The scale coefficient is 40.
The parameters of the indexing are listed below:
Permissible angle error, deg.: 0.050
Number of solutions: 10
Solution N:
1: Mn = 41.384, V = 744.47
2: Mn = 30.727, V = 354.78
3: Mn = 30.205, V = 614.03
4: Mn = 28.929, V = 460.42
5: Mn = 28.567, V = 836.77
6: Mn = 27.690, V = 282.25
7: Mn = 27.192, V = 564.49
8: Mn = 24.889, V = 322.12
9: Mn = 24.326, V = 644.25
10: Mn = 22.492, V = 701.39
Index sum |h| + |k| + |l| < 5
Indexes to search for an approximate solution:
hmax = 1; kmax = 1; lmax = 2
Permissible error Delaunay conversion: 0.50

Best fit:
Crystal system: orthorhombic
Bravais cell: Primitive (P)

Parameters of elementary cell:
a = 5.2695 (29)
b = 15.602 (18)
c = 9.0568 (54)
V = 744.60 (80)

Table S7.1. Comparison of position of peaks (2T) in SAXS pattern in deg., distance (d) between crystal planes between o – experiment and c – calculated. Calculated SAXS intensity (I). Miller indices (h, k, l)

N	2To	2Tc	2Tc-2To	do	dc	do-dc	I	h	k	l
1	11.2800	11.2839	-0.0039	7.83545	7.83275	0.00271	20000.0	0	1	1
2	17.7400	17.7457	-0.0057	4.99406	4.99247	0.00160	10000.0	1	1	0
3	19.5600	19.5812	-0.0212	4.53329	4.52842	0.00487	30000.0	0	0	2
4	22.8000	22.7731	0.0269	3.89588	3.90043	-0.00455	15000.0	0	4	0
5	31.7000	31.7462	-0.0461	2.81946	2.81547	0.00399	25000.0	0	2	3
6	36.2500	36.1303	0.1197	2.47532	2.48325	-0.00793	35000.0	1	2	3
7	39.3700	39.5265	-0.1565	2.28604	2.27735	0.00869	40000.0	2	0	2
8	45.1600	45.1411	0.0189	2.00548	2.00627	-0.00079	20000.0	1	5	3
9	49.3000	49.3249	-0.0249	1.84632	1.84544	0.00087	100000.0	1	6	3

10	54.6000	54.6659	-0.0659	1.67895	1.67708	0.00187	20000.0	2	2	4
11	61.3500	61.3469	0.0031	1.50941	1.50947	-0.00007	95000.0	0	0	6
12	64.8000	64.8012	-0.0012	1.43713	1.43710	0.00002	100000.0	3	6	1
13	71.4000	71.3947	0.0053	1.31962	1.31970	-0.00009	95000.0	3	7	2
14	92.6000	92.5679	0.0321	1.06513	1.06541	-0.00029	2000.0	4	0	5

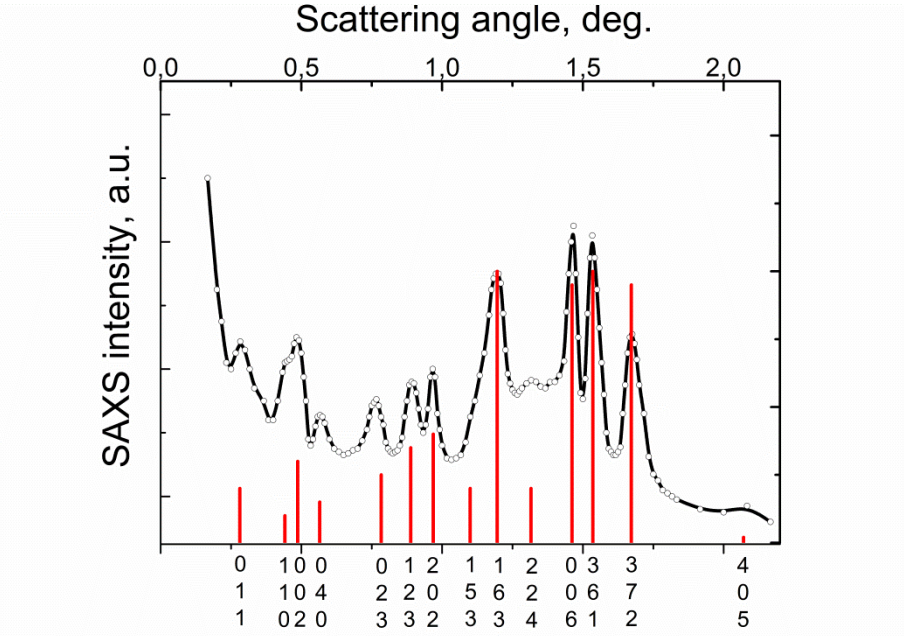

Figure S7.1 – Calculated peaks (red lines) and SAXS pattern (black line) of $SS_{4.6}$.

Rescaling procedure results in the $SS_{4.6}$ cell parameters:
a = 21.1 nm;
b = 62.5 nm;
c = 36.2nm.

The same approximation was done for the sample $PbS_{6.7}$.
Best fit:
Crystal system: orthorhombic
Bravais cell: Primitive (P)

Table S7.2. Comparison of position of peaks (2T) in SAXS pattern in deg., distance (d) between crystal planes between o – experiment and c – calculated. Calculated SAXS intensity (I). Miller indices (h, k, l)

N	2To	2Tc	2Tc-2To	do	dc	do-dc	I	h	k	l
1	8.6860	8.6384	0.0476	10.17470	10.23067	-0.05597	13000.0	0	0	1
2	17.4200	17.3264	0.0936	5.08805	5.11533	-0.02729	52000.0	0	0	2
3	21.0700	21.0807	-0.0107	4.21416	4.21204	0.00212	6500.0	1	0	1
4	26.2400	26.1161	0.1239	3.39440	3.41022	-0.01582	8700.0	0	0	3
5	28.6500	28.5909	0.0591	3.11412	3.12042	-0.00631	4500.0	1	1	2
6	32.4500	32.6138	-0.1638	2.75760	2.74412	0.01348	5500.0	1	0	3
7	35.7900	35.7914	-0.0014	2.50754	2.50744	0.00010	5600.0	0	3	0
8	40.6600	40.6776	-0.0176	2.21773	2.21682	0.00092	31000.0	1	2	3
9	44.2700	44.2420	0.0280	2.04491	2.04613	-0.00123	16000.0	0	0	5
10	47.4500	47.5009	-0.0509	1.91501	1.91308	0.00193	11000.0	2	0	3
11	62.1600	62.1317	0.0283	1.49254	1.49315	-0.00061	2800.0	3	1	1

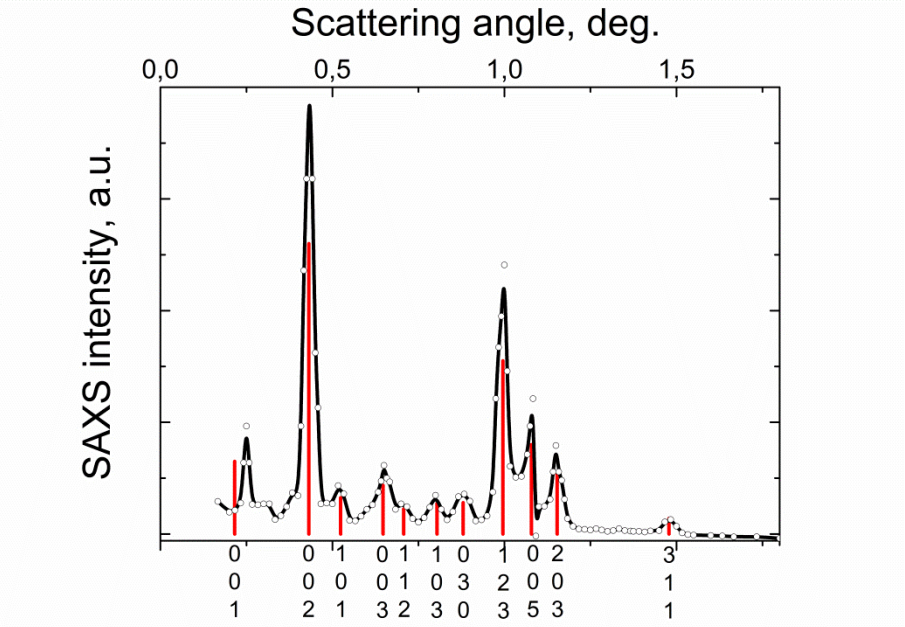

Figure S7.2 – Calculated peaks (red lines) and SAXS pattern (black line) of $SS_{6.7}$.

Rescaling procedure results in the $SS_{6.7}$ cell parameters:
a = 18.5 nm;
b = 30.1 nm;
c = 40.9 nm.

S8. Optical and SEM images of superstructures

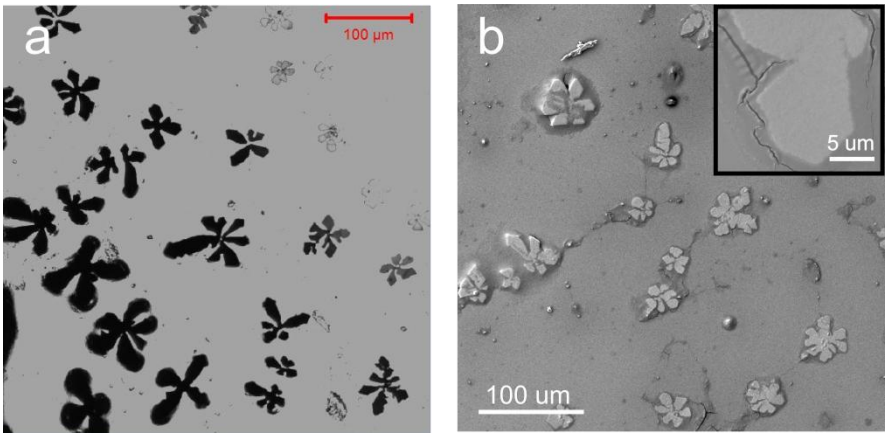

Figure S8.1 – Optical microphotograph (a) and SEM image (b) of $SS_{4.6}$

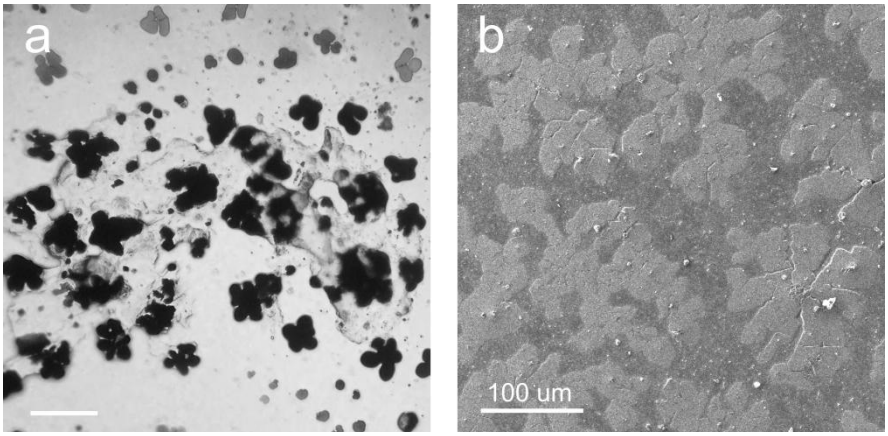

Figure S8.2 – Optical microphotograph (a) and SEM image (b) of $SS_{6.7}$. Scale bar in (a) is of 100 um

From optical microphotographs it can be seen that the size of superstructures differs through the sample. The size of superstructures strongly depends on the local CQD concentration and hence on the number of "available" CQDs in the solution. In the case of $SS_{4.6}$, the CQD concentration increases from the center of the cell to the edges (Fig.S8.1(a)). In the case of $SS_{6.7}$ the local CQD concentration is greater in the vicinity of the defect on the substrate (Fig.S8.2(a)).

The obtained structures are very prone to destruction. This is evident from the SAXS patterns in Fig.5 and also confirmed by SEM images of $SS_{4.6}$ and $SS_{6.7}$ (Fig.S8.1 (b) and FigS8.2 (b), respectively). Since superstructures were obtained on a non-conducting substrate, it was necessary to cover them with various conducting materials to obtain SEM images. After covering procedure the superstructures did not change their shape, but they "pressed" against the substrate.

S9. Estimation of the mean size of the crystalline regions in superstructures

The broadening of the peak in SAXS pattern is related to the size of area with the crystalline structure in solid. This relation can be fitted by the Scherrer equation:

$$L_{SS} = \frac{k \cdot \lambda}{\Delta(2\vartheta)\cos(\vartheta)}, \quad (3)$$

where L_{SS} is the mean size of the ordered areas in solid; k is a shape factor equal to 1; λ is the X-ray wavelength, λ = 1.54 A; θ is the scattering angle.

Table S9. Calculating domain sizes

Sample name	Peaks in SAXS pattern							
$SS_{4.6}$	Peak position, 2θ, deg.	0.75	0.88	0.97	1.2	1.46	1.53	1.67
	Peak width, Δ(2θ), deg.	0.06	0.035	0.025	0.07	0.035	0.025	0.06
	L_{SS}, nm	152	241	353	132	165	353	152
$SS_{6.7}$	Peak position, 2θ, deg.	0.25	0.43	0.65	0.80	1.00	1.08	1.15
	Peak width, Δ(2θ), deg.	0.03	0.035	0.06	0.07	0.05	0.025	0.06
	L_{SS}, nm	295	245	147	126	177	353	147

S10. Critical CQD concentration estimation.

Primary beam attenuation coefficient (K) at 0 degrees can be calculated as:

$$K = I_0/I_{exp} = e^{-\mu d}$$

where I_0 is the intensity of the primary beam before the sample compartment, I_{exp} is the intensity of the primary beam after the sample, d is the sample thickness, and μ is the coefficient of linear attenuation. Measurement of the I_{exp} intensity makes it possible to control the thickness of the solution layer, and therefore the change in the QD concentration in the solution. Intensity I_{exp} was recorded before each measurement of the angular dependence. It worth to note that the evaporation of the solvent leads to the I_{exp} increasing together with the measured intensity of the scattering by the CQDs, as it is shown in Fig.S10.1.

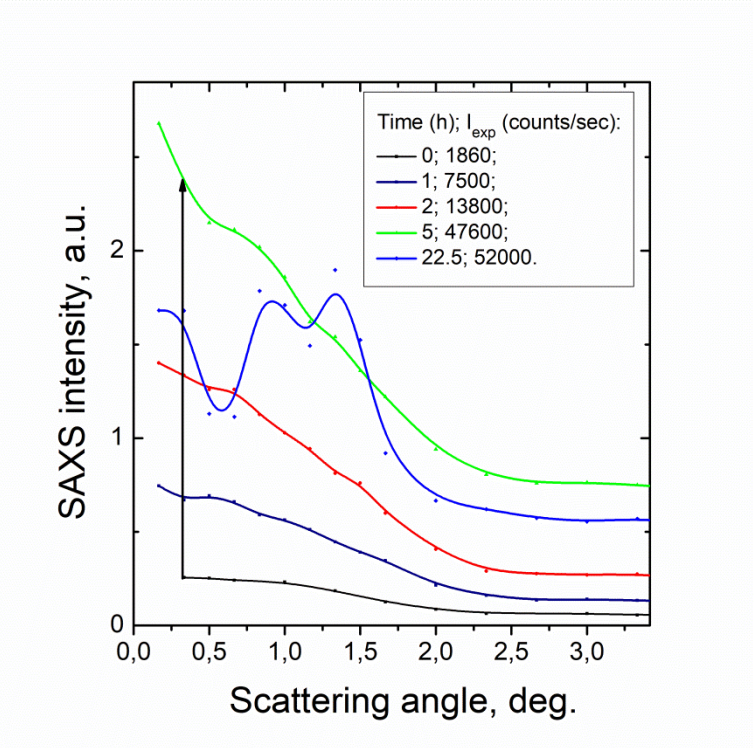

Figure S10.1. SAXS patterns for $SS_{4.6}$ formation. The inset shows the corresponding I_{exp} values.

For tetrachloromethane (CCl_4), the coefficient of linear attenuation, μ, is of 163 cm^{-1}. At the beginning of the experiment the solution thickness was 0.33 mm and the K coefficient is approximately 200. The thickness of the CQD solution in cuvette was calculated by the above mentioned equation and presented in Fig.S10.2.

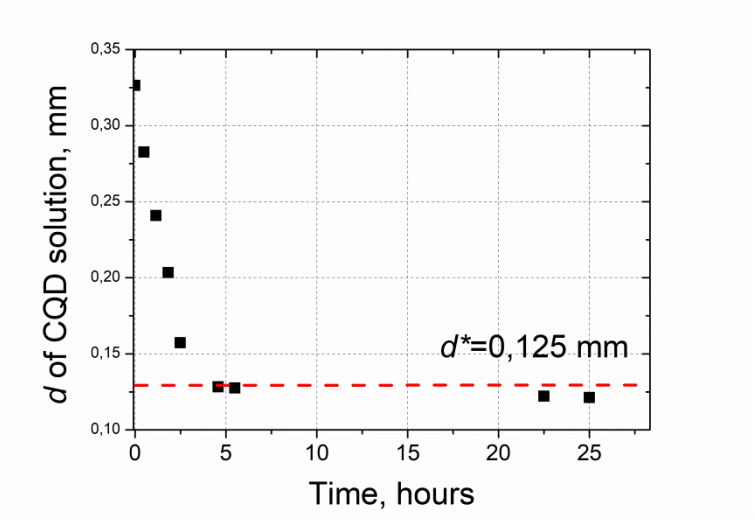

Figure S10.2. The dependence of the calculated thickness of the $CQD_{4.6}$ solution, *d*, with time.

The CQD assembly process starts from the solution thickness of 0.125 mm. From this value the CQD concentration (*C*) can be estimated taking into account initial concentration and solution volume. The *C* decreases from $5 \cdot 10^{-5}$ M to $1.3 \cdot 10^{-5}$ M. This contributes to the CQD volume fraction equal to 0.2%. With further CQD assembly and solvent evaporation CQD volume fraction increases up to 1% for $SS_{4.6,}$ estimated from the crystal lattice parameters.

S11. Optical properties of superstructures compared to CQD solutions

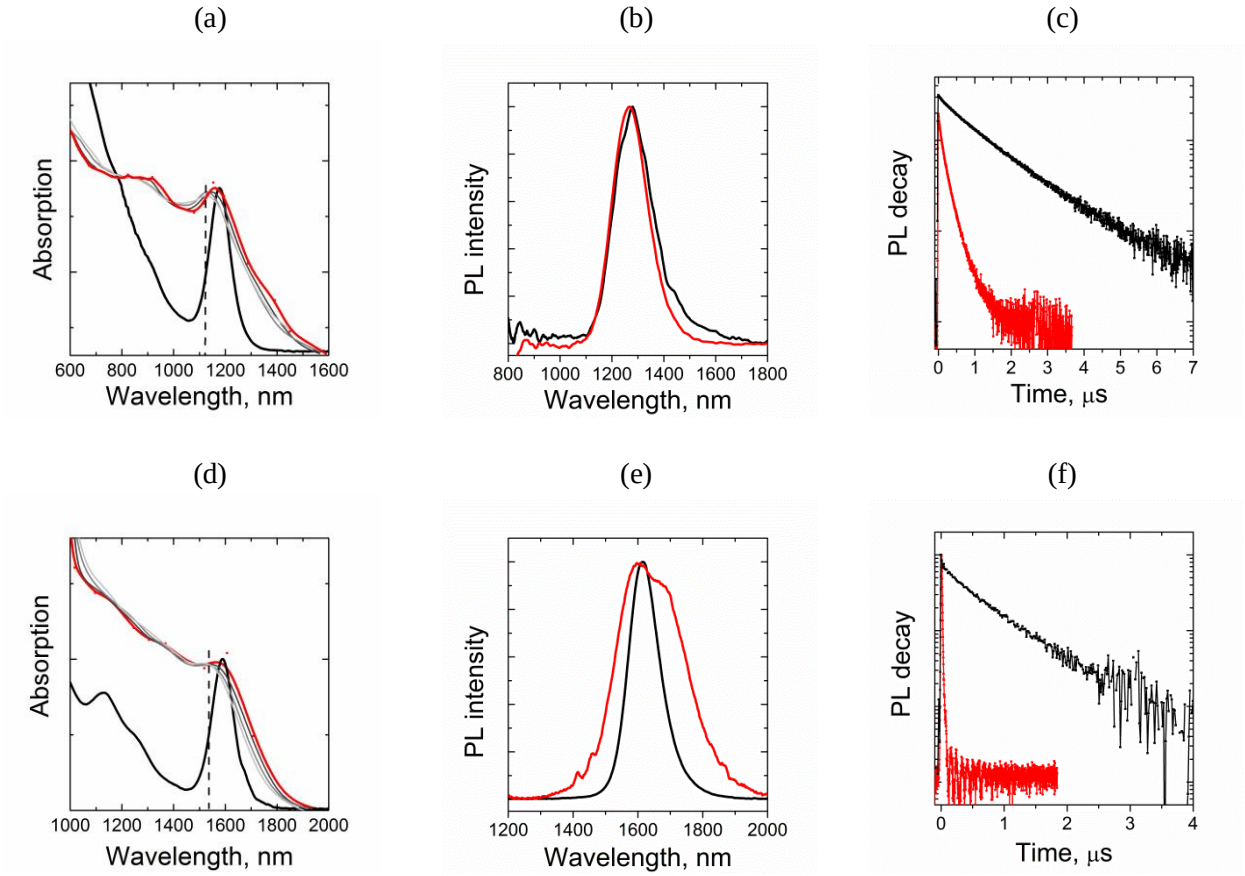

Figure S11 – Optical properties of CQD solution in TCM (black curves) and SS (red curves) of QDs with D = 4.6 nm (a)-(c), 6.7 nm (d)-(f);
(a) and (d) - ABS spectra; (b) and (e) - PL spectra; (c) and (f) - PL decay.
In (a) and (d) SS absorption spectra are presented after 3 months (dark grey), 6 months (grey) and 1 year (light grey); dashed line is the ABS peak position after 1 year.